Biomimetic Pattern Transfer**

By *Li-Qun Wu*, *Reza Ghodssi*, *Yossef A. Elabd*, and *Gregory F. Payne**

Biological systems routinely use phenols to construct complex materials with diverse functions. Typically, these phenolic materials are generated using oxidative enzymes to initiate a cascade of uncatalyzed reactions. We mimic these processes to micropattern films of the aminopolysaccharide chitosan. Specifically, we microfabricate silicon wafers to have gold patterns, cast a chitosan film onto the patterned wafers, and commence pattern transfer by polarizing the underlying gold surfaces to electrochemically initiate the phenol reaction cascade. The electrochemically initiated reactions lead to modification of the chitosan film's chemistry, structure, and fluorescence. Further, electrochemically initiated modification of the chitosan film is localized to the interfacial region between the film and the anode, with resolution in the lateral direction of at least 20 μm. These results demonstrate that electrochemical pattern transfer provides a promising new method for micropatterning flexible films.

1. Introduction

Nature is well known for its use of enzymes to catalyze reactions with exquisite selectivity. Surprisingly, nature uses enzyme-initiated processes that offer much lower fidelity to construct a variety of functionally important materials. In these processes, enzymes oxidize a precursor into an activated intermediate that undergoes a cascade of uncatalyzed reactions. Typically, the precursors are phenolics, the initiating enzymes are peroxidases, laccases, or phenol oxidases, and the resulting materials have a diversity of functional properties. Both the reaction cascades and the resulting materials are complex and incompletely understood,[1,2] yet the importance of these materials in nature is illustrated by a few examples.

Melanins are a complex group of phenolic polymers that may be best known for their optical properties.[3,4] Depending on which phenols are used for their synthesis, the melanins have a variety of colors and are responsible, at least in part, for the coloration of the butterfly's wings,[5] the chicken's feathers,[6] and the lion's mane.[7] Their UV-absorbing properties suggest that melanins serve photoprotection functions[8,9] while their photon–phonon coupling suggests a potential role for thermoregulation.[10] In addition to their optical properties, there are a number of reports that melanins offer interesting electrical properties. Thirty years ago, melanins were reported to behave as amorphous semiconductors,[11,12] and these reports have stimulated a handful of recent studies.[13,14] Also, bacteria have been reported to synthesize quinones[15] and melanins[16,17] that serve as extracellular electron carriers to support anaerobic respiration.

There are several biological examples in which reactions of natural phenols yield materials that serve important mechanical functions. Most familiar is lignification, where plant phenols are polymerized into a complex three-dimensional crosslinked network. Also, insect's harden their cuticle in a "tanning" process that is initiated by the enzymatic oxidation of catecholic compounds.[18,19] A final example is the mussel's adhesive protein that "sets" when some of its phenolic amino acid residues (e.g., tyrosine or dihydroxyphenylalanine residues) are enzymatically oxidized to initiate protein crosslinking that confers cohesive strength.[20,21]

There have been some efforts to mimic these natural processes to generate functional materials.[22–28] However the broader use of such biomimetic approaches will require an ability to control the reaction cascades. In nature, the reaction cascades are controlled at the initiation stage and often control is achieved by compartmentalization (the reactants and initiating enzymes are spatially separated within the cell)[29–31] or by the conversion of inactive pro-enzymes.[32–34] Compartmentalization and enzyme activation may not be the most convenient methods to control initiation of these reaction cascades in vitro. Here, we initiate the phenol reaction cascade by electrochemical oxidation and use microfabricated electrodes to spatially and temporally control initiation. Once initiated, the reaction cascade is exploited to chemically modify a polysaccharide film.

[*] Prof. G. F. Payne, Dr. L.-Q. Wu
Center for Biosystems Research, University of Maryland
Biotechnology Institute, 5115 Plant Sciences Building
College Park, MD 20742 (USA)
E-mail: payne@umbi.umd.edu
Prof. R. Ghodssi
Department of Electrical and Computer Engineering
University of Maryland at College Park
College Park, MD 20742 (USA)
Prof. Y. A. Elabd
Department of Chemical Engineering, Drexel University
3141 Chestnut St., Philadelphia, PA 19104 (USA)
Prof. G. F. Payne
Department of Chemical and Biochemical Engineering
University of Maryland
Baltimore County, 1000 Hilltop Circle, Baltimore, MD 21250 (USA)
Prof. R. Ghodssi
The Institute for Systems Research
University of Maryland at College Park
College Park, MD 20742 (USA)

[**] Financial support for this work was provided by the United States Department of Agriculture (2001-35504-10667), the National Science Foundation (grant BES-0114790). The authors would like to gratefully acknowledge Anthony Lowman and Jonathon Thomas at Drexel University for their help with tensile-test measurements.

 DOI: 10.1002/adfm.200400279

2. Results and Discussion

2.1. Chemical Modification of Chitosan by Electrochemically Initiated Reactions

Figure 1a outlines the electrochemically initiated pattern transfer operation. Standard microfabrication methods are used to pattern gold onto a silicon wafer. A film of the aminopolysaccharide chitosan is then coated on top of the wafer and then neutralized (these films are stable and can be extensively washed because chitosan is insoluble above a pH of 6.5). This chitosan-coated wafer is immersed in a solution containing a phenol, and the reaction cascade is initiated by polarizing the anode to electrochemically oxidize the phenol into the reactive intermediates. By analogy to the enzymatic oxidation of phenols, the reactive intermediates generated at the anode are expected to react with the aminopolysaccharide chitosan.[35–37] Compared to other polysaccharides, chitosan is uniquely reactive because it has nucleophilic primary amino groups at nearly every repeating sugar residue (i.e., electrochemical pattern transfer may not apply to the patterning of polysaccharides such as hyaluronic acid[38] and alginate[39] that lack nucleophilc moieties).

Evidence that electrochemically initiated reactions result in the chemical modification of chitosan was obtained by examination of the films after they were peeled from the wafer. A photograph of the film in Figure 1b shows that the unpatterned region remains transparent, while the region patterned (i.e., modified) with the phenol catechol appears dark. The UV-vis spectra of this film show that the unpatterned region has no peaks, while the patterned (i.e., modified) region has a broad UV-vis absorbance and a peak at 430 nm. These observations are consistent with spectra for phenolic oxidation products[2,40] and for oxidation products that have reacted with chitosan.[37]

As illustrated in Figure 2a, if the reactive intermediates generated at the anode diffuse away slowly compared to their rate of reaction with the chitosan film, then chitosan chains in the vicinity of the anode will be preferentially reacted. Attenuated total reflectance Fourier-transform infrared (ATR-FTIR) spectroscopy was used to provide chemical evidence for the spatial localization of electrochemically initiated reactions of the chitosan films. A single-reflection diamond ATR probe with a 100 μm tip was placed on the modified and unmodified surface regions of the films. This pseudo-surface technique profiles approximately 1 μm into the 40 μm thick chitosan film. Figure 2b shows the IR spectra for the unpatterned and patterned (modified) regions of the "proximal" surface of the chitosan film — the surface that had been in direct contact with the wafer. As illustrated by the arrows, there are three IR bands of interest that appear in regions for the stretching vibrations of the pro-

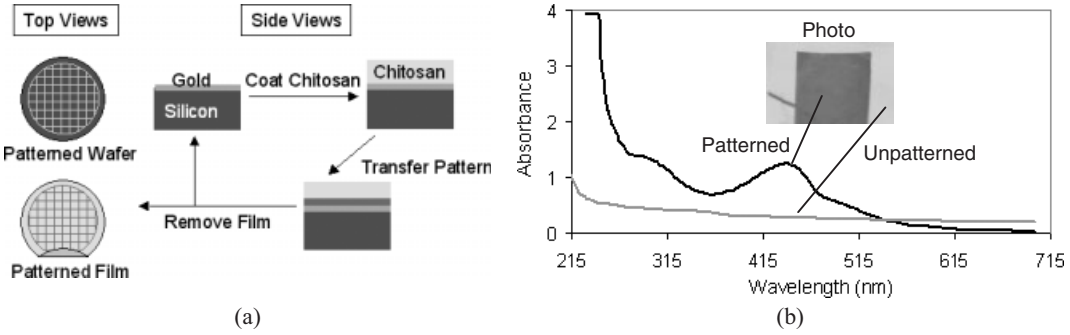

Figure 1. Evidence that electrochemically initiated reactions chemically modify chitosan films. a) Standard microfabrication methods are used to pattern gold features onto a silicon wafer and these features are electrochemically transferred to films of the polysaccharide chitosan. b) Photograph and UV-vis spectra of dip-cast chitosan films patterned with catechol (6 mM for 6 min) and peeled from the wafer.

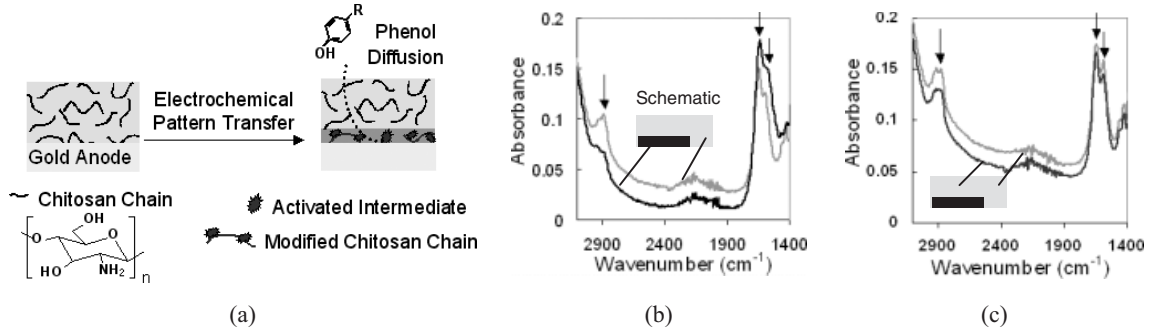

Figure 2. Chemical evidence that pattern transfer is spatially localized. a) Electrochemical pattern transfer requires that phenols diffuse through the chitosan film to be oxidized at the anode surface, and the resulting reactive intermediates undergo reaction with chitosan chains adjacent to the anode. For simplicity, chitosan is shown as a glucosamine homopolymer while it is formally a co-polymer with some *N*-acetylglucosamine residues. ATR-IR spectra of the b) proximal and c) distal surfaces of a chitosan film modified with catechol (6 mM for 6 min).

ADVANCED FUNCTIONAL MATERIALS

tonated amine ($-NH_3^+$), carbonyl (–NH–C=O), and amine ($-NH_2$) at 2886, 1643, and 1593 cm^{-1}, respectively.[41,42] The distinct changes in the IR spectra (peak shifting and loss in intensity) in the amine and protonated amine stretching vibrations relative to the carbonyl group indicate that catechol oxidation products undergo covalent bond formation with chitosan's amines. Figure 2c shows the IR spectra for the unpatterned and patterned regions of the "distal" surface of the chitosan film — the surface exposed to the solution during electrochemical pattern transfer. There is no clear difference between the two spectra demonstrating that electrochemical pattern transfer is confined to the proximal surface of the chitosan films.

2.2. Localization of Electrochemical Modification

Physical evidence that electrochemical modification of chitosan films can be spatially localized was provided by examination of a film's surface profile. For this study, a silicon wafer was patterned to have two independent sets of gold surfaces (gold thickness of 0.2 μm). As illustrated in Figure 3a, only the upper set of gold surfaces can be polarized to serve as electrodes. A thin (1 μm) chitosan film was spin-cast on top of the micropatterned wafer and neutralized. The chitosan-coated

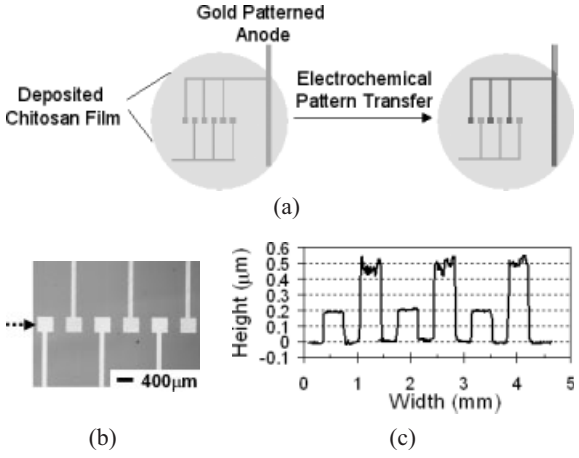

Figure 3. Physical evidence that electrochemical modification is localized to regions of chitosan adjacent to the anode. A thin chitosan film (1 μm) was spin-cast onto the patterned wafer, and electrochemically modified with catechol (3 mM for 6 min). After rinsing, the chitosan-coated wafer was dried and analyzed. a) Schematic of patterned wafer showing two independent sets of gold surfaces (only the upper surfaces can be polarized to serve as anodes). b) Photomicrograph of chitosan-coated wafer after electrochemically initiated reaction. c) Surface profile of modified chitosan film.

wafer was then immersed in a solution containing catechol, and a positive voltage was applied to the polarizable gold surfaces to initiate the reaction cascade. As illustrated in Figure 3a, we anticipate that chitosan will be modified in the regions of the film directly adjacent to the anode.

After electrochemical reaction, the chitosan-coated wafer was rinsed with distilled water, air-dried overnight, and then examined (the film was not removed from the silicon wafer in this experiment). The photomicrograph of Figure 3b shows a slight discoloration of the transparent chitosan film in the regions above the anode surfaces. A profilometer was used to scan the surface of the chitosan-coated wafer in the direction indicated by the arrow in Figure 3b. The surface profile in Figure 3c shows that the thickness of the chitosan film changes in a reproducible fashion. The chitosan surface is elevated by 0.2 μm in the regions covering the unpolarized gold surfaces (this elevation corresponds to the thickness of the patterned gold relative to the silicon wafer). Profiles in the regions above the anodes show the surface is elevated by 0.4 to 0.5 μm due to both the gold thickness (0.2 μm) and the electrochemical reaction. In the lateral direction (i.e., the *x*-axis in Fig. 3c), the lengths of the elevated regions are approximately 400 μm corresponding to the dimensions of the gold squares patterned on the silicon wafer (note the orders of magnitude differences in length scales of the two axes in Fig. 3c). The results in Figure 3c provide physical evidence that the electrochemically initiated reactions lead to changes in the chitosan film and these changes are localized to regions adjacent to the anode.

2.3. Property Changes Conferred by Electrochemical Modification

As mentioned, nature commonly exploits phenol reaction cascades in the construction of materials — although proposed structures and functions of these materials are sometimes controversial. We explored how the electrochemical modification of chitosan films affects three properties.

The first property examined was conductivity. Samples were prepared for this study by dip-casting chitosan films onto an unpatterned gold-coated wafer, electrochemically modifying the films with various natural phenols, peeling the films from the wafer and cutting samples for analysis by impedance spectroscopy. Figure 4 shows a complex impedance plot for both unmodified chitosan films and films electrochemically modified with various natural phenols. Typical behavior is shown in Figure 4, where there are two well-defined regions: a semi-circular region in the high frequency zone and a linear region in the low frequency zone. Resistance (R_b) was determined from the intercept of the real (Z') axis by an extrapolation method[43] and conductivity was calculated from $\sigma = 1/(R_b A)$, where l is the length of the film and A is the cross-sectional area. The tabulated data in Figure 4 shows that there is a decrease in conductivity (i.e., an increase in resistance) when the films are electrochemically modified. Conductivity in chitosan is due to either electron or OH^--ion mobility via protonated amine sites (NH_3^+).[44] Since electrochemical modification of chitosan consumes amines, there are fewer sites available, resulting in lower conductivity in the modified films. Thus, electrochemical modification alters the conductivity of chitosan films.

The examination of two additional properties of electrochemically modified chitosan films was motivated by an analogy to the insect cuticle. The insect's cuticle is a composite material consisting of chitin fibers embedded within a protein

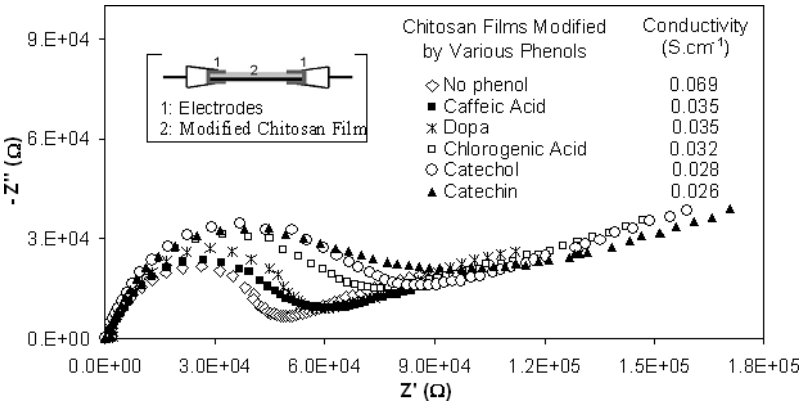

Figure 4. Conductivity changes of electrochemically modified chitosan films. Plot of imaginary impedance ($-Z''$) versus real impedance (Z') for chitosan film, and films electrochemically modified with various natural phenols (6 mM for 20 min, dihydroxyphenylalanine is abbreviated Dopa). Films (3 cm × 0.5 cm and 40 μm thick) were analyzed as illustrated in the schematic. The bulk resistance and conductivity were calculated as described in the text.

matrix and these components appear to be crosslinked through quinone-mediated reactions. (Interesting to note is that chitosan is derived from chitin by partial deacetylation of chitin's repeating *N*-acetylglucosamine residues). In some cases, spatial differences in cuticle structure, composition and properties are believed to be important for function. For instance, several recent studies have examined how the vein pattern in the insect's wing affects the wing's response to applied forces.[45,46] We examined whether electrochemical modification of chitosan affects the film's mechanical properties and if electrochemical patterning can be performed over a broad surface.

Using mild modification conditions, we electrochemically patterned a 2 mm stripe from catechol onto a 10 mm wide chitosan film (40 μm thickness) and examined the tensile properties of this film. Figure 5 compares the stress–strain curve for this patterned chitosan film with the curve for an unpatterned

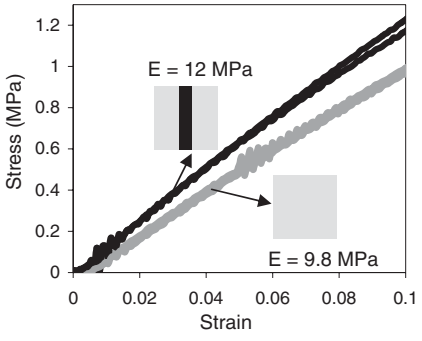

Figure 5. Electrochemical modification increases the film's mechanical properties. Tensile tests (10 mm × 10 mm film of 40 μm thickness) were performed to compare the behavior of an unmodified chitosan film with a chitosan film that had been electrochemically patterned with catechol (5 mM for 20 min) to have a 2 mm stripe (films were tensile-tested in water at 37 °C).

chitosan film. Films with this single phenolic stripe were observed to have a Young's modulus 20 % higher than an equivalent unpatterned film (12 vs. 9.8 MPa). Chitosan films could be patterned over larger areas; Figure 6a shows that we fabricated silicon wafers to have either a series of 100 μm parallel lines or a mesh of 100 μm lines. To facilitate visual observation, we used relatively high catechol concentrations (30 mM) and long

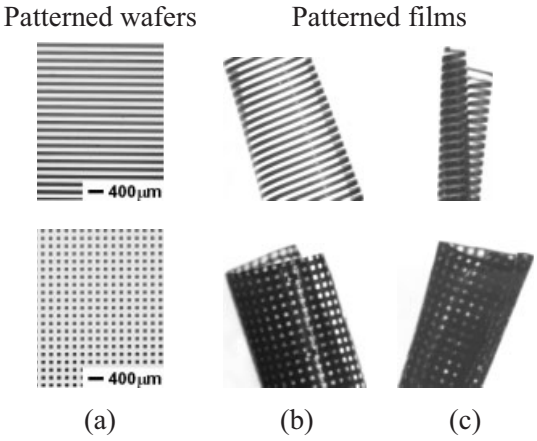

Figure 6. Electrochemical patterning over an extended area. a) Photomicrographs of gold-patterned silicon wafers (100 μm line widths). b,c) Photomicrographs of chitosan films patterned using catechol (30 mM for 40 min).

reactions times (40 min) so the modified regions would be darker. After reaction, the chitosan films were peeled from the wafer and observed. The photomicroscopic images in Figure 6b show that the patterns were transferred as darkened regions onto the transparent chitosan films. These results show that pattern transfer is achieved with high fidelity over relatively large areas, and that the films remain flexible.

Portions of the insect cuticle have also been reported to be fluorescent.[47] In fact, fluorescence is common for materials generated from phenols. For instance, melanins are reported to be responsible for the fluorescence in the retinal pigment epithelium,[48,49] melanins derived from opioid peptides are fluorescent,[50] and oxidation products formed from reactions between the natural phenol catechin and amines are fluorescent.[51] We examined the fluorescent properties of chitosan films electrochemically modified with catechin.

To test for fluorescence, we cast a chitosan film onto an unpatterned gold-coated wafer and reacted the film with catechin. After reaction, the modified chitosan film was removed from the wafer and rinsed extensively with water and ethanol. The modified chitosan film was visually observed to be light brown in color. When viewed using a fluorescence microscope

ADVANCED FUNCTIONAL MATERIALS

(excitation filter 425±30 nm and an emission barrier filter of 480 nm), the catechin-modified chitosan film was observed to be bright green. The UV-vis spectrum of the catechin-modified chitosan film shows an absorption maximum at 410 nm (not shown). Figure 7 shows the fluorescence emission spectra of the catechin-modified chitosan film that was illuminated at an excitation wavelength of 410 nm. An emission band is observed at about 490 nm. It should be noted that no fluorescence was observed in controls consisting of either a solution of unreacted catechin or a chitosan-coated wafer that was contacted with catechin but without being oxidized. Thus, the result in Figure 7 shows that electrochemical modification with catechin confers fluorescence to the chitosan film.

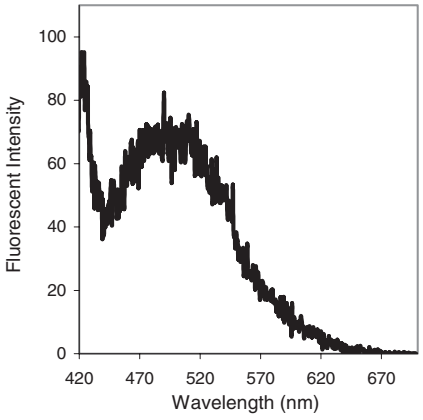

Figure 7. Fluorescence emission spectra of chitosan film electrochemically modified with catechin. Films were electrochemically modified with catechin (3 mM for 6 min), peeled from the wafer, rinsed with water and ethanol, and examined with an excitation wavelength of 410 nm/10 nm bandpass.

2.4. Spatial and Temporal Control of Electrochemical Pattern Transfer

The fluorescence of the catechin-modification reaction provides a convenient method to study the resolution of electrochemical patterning of chitosan films. The spatial resolution of pattern transfer was first examined using the mesh pattern in Figure 8a (this is the same patterned wafer as in Fig. 6a). The fluorescence photomicrographs in Figures 8b show that a fluorescent mesh is observed in the regions that underwent anodic oxidation (shown as light green in the fluorescence photomicrographs). These fluorescent regions are well resolved from the non-fluorescent 100 μm squares (shown as dark regions). These results indicate that electrochemical pattern transfer can be spatially resolved over relatively large surfaces.

To further demonstrate that electrochemical micropatterning on chitosan films can be controlled spatially and temporally, we created a gold patterned wafer as illustrated in the Figure 9a. This pattern consists of thin lines (20 μm) that could be independently polarized from four separate leads. Chitosan was dip-cast on top of these patterned lines and four sequential pattern transfer steps were performed (the chitosan was not removed from the wafer during this experiment). In the first pattern transfer step, the chitosan-coated wafer was immersed in a catechin solution and the voltage was applied to the top lead, which is connected to the rightmost gold line. After this reaction, the wafer was removed from the catechin solution and examined using a fluorescence microscope. The first fluorescence photomicrograph and image analysis in Figure 9b shows that a single fluorescent line with a width of 20 μm was patterned onto the film. For the second pattern transfer step, this same chitosan-coated wafer was again contacted with a catechin solution and a voltage was applied to the second lead to polarize the second gold line (second from the right). After reaction and rinsing, the chitosan-coated wafer was again examined and the fluorescence photomicrograph in Figure 9b shows a second fluorescent line had been transferred onto the chitosan film during this second pattern-transfer step. Similar steps were performed to transfer a third and fourth fluorescent lines to the chitosan. The results in Figure 9 show that electrochemical pattern transfer can be spatially controlled to resolutions of at least 20 μm (this is the resolution limit for our photolithographic gold-patterning technique). Also, the results in Figure 9 indicate that electrochemical pattern transfer can be controlled temporally based on when the electrode is polarized. Finally, we should note that in an analogous experiment we observed that we could sequentially pattern different phenols (e.g., catechol, caffeic acid, and chlorogenic acid) onto the chitosan film. Photomicrographs of these films are not as illustrative as those of Figure 9 because films modified with these other phenols are not fluorescent.

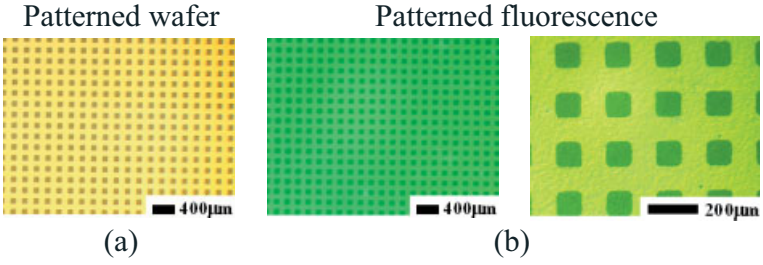

Figure 8. Fluorescence micropatterning of chitosan film. a) Optical photomicrograph showing the gold mesh pattern on the silicon wafer (100 μm line widths). b) Fluorescence photomicrographs of chitosan-coated silicon wafer after electrochemical pattern transfer with catechin (3 mM for 6 min).

3. Conclusion

We mimic natural processes to controllably transfer patterns from a microfabricated surface to a flexible film of the polysaccharide chitosan. Pattern transfer is achieved by polarizing micropatterned gold electrodes to initiate an oxidative reaction cascade that modifies chitosan's chemistry, structure, and properties. Potentially, these reactions could be exploited to micropattern unique chemical functionalities (e.g., carboxylic or alkyl groups) onto the film's surface to provide localized reactive sites, or to

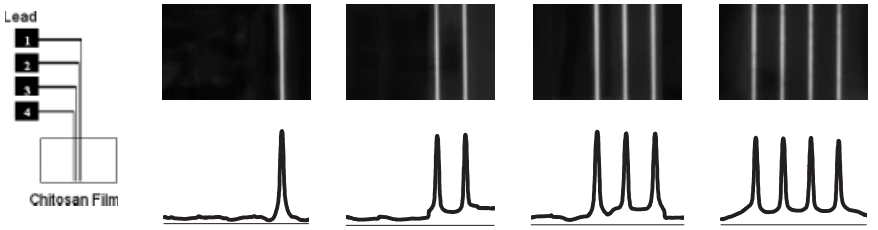

Independent electrodes to sequentially pattern 20 μm lines
(a)
(b)

Figure 9. Spatial and temporal control of electrochemical micropatterning. a) Scheme illustrating our patterned surface with four electrically independent 20 μm gold lines. b) A series of fluorescence photomicrographs showing sequential pattern transfer using catechin (3 mM for 6 min). The fluorescence intensity profiles are shown below each image.

spatially control surface energies. Importantly, phenols are ubiquitous natural products available with diverse chemical functionalities while electrochemical oxidation may provide a generic means to initiate pattern transfer. Further, the results suggest that large regions of chitosan can be patterned to generate flexible films with spatially varying (e.g., anisotropic) properties.

4. Experimental

Chitosan was reported by the supplier (Sigma–Aldrich) to have a degree of acetylation of 15 % and a molecular weight of 200 000 (no effort was made to assess the effects of these variables). This polysaccharide was dissolved in acidic solution as described elsewhere [52]. Gold was patterned onto silicon wafers using standard photolithographic methods [52] and the wafers were cut into appropriate sizes for each experiment (we use the term "wafer" throughout to refer to both the intact wafer and the cut pieces used in individual experiments).

Chitosan was coated onto patterned wafers by either spin-casting (for thin films of ≈1 μm) or dip-casting (for thicker films of ≈40 μm that could be peeled from the wafer). After casting the solution (2.5 wt.-% chitosan), the films were dried at 40 °C for 2 h, and then the chitosan-coated wafer was neutralized in NaOH (1 M) for 5 min and then rinsed extensively with distilled water. No effort was made to control the chitosan film's thickness. For electrochemical pattern transfer, the chitosan-coated wafer was immersed in a 20 mM phosphate buffer (pH 6.5) containing a phenol (the type and concentration varied). Pattern transfer was initiated by polarizing the patterned gold surface (i.e., the anode) using a direct current (DC) power supply (Agilent 6614C) to achieve a constant current density 0.2 mA cm^{-2}. An unpatterned gold-coated wafer served as the cathode for this electrochemical reaction. After the reaction, the wafer was disconnected from the power supply, removed from the phenol solution and rinsed with distilled water.

Chemical analyses of the electrochemically modified chitosan films were performed using UV-vis spectrophotometry (Spectronic Genesys) and attenuated total reflectance Fourier-transform infrared spectroscopy (ATR-IR; Nicolet Nexus 870 FTIR spectrometer equipped with a single-reflection diamond ATR objective from Spectra-Tech Infinity Series). The UV-vis absorbance of chitosan films was measured by placing the film perpendicular to the light path. IR surface analysis was performed by providing intimate contact between the ATR objective (refractive index = 2.73; 100 μm tip) and the chitosan film surface. All IR spectra were collected using 32 scans with a 4 cm^{-1} resolution.

The patterned wafers and patterned chitosan films were examined using an optical microscope (Model FS70, Mitutoyo Corp.) with a digital camera (Nikon DXM 1200). In some cases, we used a fluorescence stereomicroscope (MZFLIII, Leica) with a fluorescence filter set (excitation filter 425 ± 30 nm and barrier filter 480 nm) and a digital camera (Spot 32, Diagnostic Instruments). These filters were chosen based on excitation/emission spectra observed for a catechin-modified chitosan film using a luminescence spectrometer (LS 55, Perkin–Elmer Instruments). Surface profile of a thin (1 μm) spin-cast chitosan film was measured using a profilometer (Alpha-step 500 Surface Profiler, TENCOR Instruments).

Alternating current (AC) impedence spectroscopy (Solartron SI 1287 Electrochemical Interface, SI 1260 Impedance/Gain-phase Analyzer, Scribner Associates, Inc.) was used to determine conductivity. Samples were prepared by dip-casting chitosan onto an unpatterned gold-coated wafer, performing electrochemical reactions with various phenols, peeling the modified film from the wafer, and cutting the film into 3 cm × 0.5 cm rectangular pieces that were approximately 40 μm thick. All conductivity measurements were performed in the plane of the film with a two-electrode technique (as illustrated in the inset in Fig. 4) under equilibrated hydrated conditions at room temperature.

Tensile testing (Instron 4442) was performed with films that had been spin-cast, electrochemically modified, peeled from the wafer and cut into 30 × 10 cm pieces that were 40 μm thick. This tensile mechanical measurement was performed in a water bath at 37 °C.

Received: June 25, 2004
Final version: August 26, 2004

[1] K. B. Stark, J. M. Gallas, G. W. Zajac, M. Eisner, J. T. Golab, *J. Phys. Chem. B* **2003**, *107*, 3061.
[2] Y. Il'ichev, J. Simon, *J. Phys. Chem. B* **2003**, *107*, 7162.
[3] P. A. Riley, *Int. J. Biochem. Cell Biol.* **1997**, *29*, 1235.
[4] K. McGraw, *OIKOS* **2003**, *102*, 402.
[5] P. B. Koch, B. Behnecke, R. H. French-Constant, *Curr. Biol.* **2000**, *10*, 591.
[6] J. Senar, J. Figuerola, J. Domenech, *Naturwissenschaften* **2003**, *90*, 234.
[7] P. West, C. Packer, *Science* **2002**, *297*, 1339.
[8] M. Rozanowska, T. Sarna, E. Land, T. Truscott, *Free Radical Biol. Med.* **1999**, *26*, 518.
[9] J. B. Nofsinger, Y. Liu, J. D. Simon, *Free Radical Biol. Med.* **2002**, *32*, 720.
[10] P. R. Crippa, F. Martini, C. Viappiani, *J. Photochem. Photobiol. B* **1991**, *11*, 371.
[11] J. McGinness, P. Corry, P. Proctor, *Science* **1974**, *183*, 853.
[12] J. E. McGinness, *Science* **1972**, *177*, 896.
[13] M. Jastrzebska, A. Kocot, L. Tajber, *J. Photochem. Photobiol. B* **2002**, *66*, 201.
[14] S. Gidanian, P. J. Farmer, *J. Inorg. Biochem.* **2002**, *89*, 54.
[15] D. Newman, R. Kolter, *Nature* **2000**, *405*, 94.
[16] C. E. Turick, F. Caccavo, Jr., L. S. Tisa, *FEMS Microbiol. Lett.* **2003**, *220*, 99.
[17] C. E. Turick, L. S. Tisa, F. Caccavo, Jr., *Appl. Environ. Microbiol.* **2002**, *68*, 2436.
[18] K. Kramer, M. Kanost, T. Hopkins, H. Jiang, Y. Zhu, R. Xu, J. Kerwin, F. Turecek, *Tetrahedron* **2001**, *57*, 385.
[19] M. R. Chase, K. Raina, J. Bruno, M. Sugumaran, *Insect Biochem. Mol. Biol.* **2000**, *30*, 953.
[20] L. A. Burzio, J. H. Waite, *Biochemistry* **2000**, *39*, 11 147.
[21] L. M. McDowell, L. A. Burzio, J. H. Waite, J. Schaefer, *J. Biol. Chem.* **1999**, *274*, 20 293.

[22] T. Chen, D. A. Small, L.-Q. Wu, G. W. Rubloff, R. Ghodssi, R. Vazquez-Duhalt, W. E. Bentley, G. F. Payne, *Langmuir* **2003**, *19*, 9382.
[23] K. Yamada, T. Chen, G. Kumar, O. Vesnovsky, L. D. Topoleski, G. F. Payne, *Biomacromolecules* **2000**, *1*, 252.
[24] Y. Kuboe, H. Tonegawa, K. Ohkawa, H. Yamamoto, *Biomacromolecules* **2004**, *5*, 348.
[25] B. P. Lee, J. L. Dalsin, P. B. Messersmith, *Biomacromolecules* **2002**, *3*, 1038.
[26] J. L. Dalsin, B. H. Hu, B. P. Lee, P. B. Messersmith, *J. Am. Chem. Soc.* **2003**, *125*, 4253.
[27] M. Yu, T. J. Deming, *Macromolecules* **1998**, *31*, 4739.
[28] T. J. Deming, *Curr. Opin. Chem. Biol.* **1999**, *3*, 100.
[29] A. M. Mayer, *Phytochem. Rev.* **1987**, *26*, 11.
[30] K. Vaughn, A. Lax, S. Duke, *Physiol. Plant.* **1988**, *72*, 659.
[31] J. C. Steffens, E. Harel, M. D. Hunt, *Recent Adv. Phytochem.* **1994**, *28*, 275.
[32] X. Zhao, M. Ferdig, B. Christensen, *Dev. Comp. Immunol.* **1995**, *19*, 205.
[33] J. Gillespie, M. Kanost, T. Trenczek, *Annu. Rev. Entomol.* **1997**, *42*, 611.
[34] S. Lai, C. Chen, R. Hou, *J. Med. Entomol.* **2002**, *39*, 266.
[35] L. Vachoud, T. Chen, G. Payne, R. Vazquez-Duhalt, *Enzyme Microb. Technol.* **2001**, *29*, 380.
[36] G. Kumar, P. J. Smith, G. F. Payne, *Biotechnol. Bioeng.* **1999**, *63*, 154.
[37] L. Q. Wu, H. D. Embree, B. M. Balgley, P. J. Smith, G. F. Payne, *Environ. Sci. Technol.* **2002**, *36*, 3446.
[38] K. Suh, A. Khademhosseini, J. Yang, G. Eng, R. Langer, *Adv. Mater.* **2004**, *16*, 584.
[39] C. Cassinelli, M. Morra, A. Carpi, R. Giardino, M. Fini, *Biomed. Pharmacother.* **2002**, *56*, 325.
[40] M. Yu, J. Hwang, T. J. Deming, *J. Am. Chem. Soc.* **1999**, *121*, 5825.
[41] J. Brugnerotto, J. Lizardi, F. M. Goycoolea, W. Arguelles-Monal, J. Desbrieres, M. Rinaudo, *Polymer* **2001**, *42*, 3569.
[42] D. Lin-Vien, N. B. Colthup, W. G. Fateley, *The Handbook of Infrared and Raman Characteristic Frequencies of Organic Molecules*, Academic Press, New York **1991**.
[43] Z. Osman, Z. Ibrahim, A. Arof, *Carbohydr. Polym.* **2001**, *44*, 167.
[44] Y. Wan, K. Creber, B. Peppley, V. Bui, *Polymer* **2003**, *44*, 1057.
[45] S. A. Combes, T. L. Daniel, *J. Exp. Biol.* **2003**, *206*, 2989.
[46] C. W. Smith, R. Herbert, R. J. Wootton, K. E. Evans, *J. Exp. Biol.* **2000**, *203*, 2933.
[47] S. Zill, S. F. Frazier, D. Neff, L. Quimby, M. Carney, R. DiCaprio, J. Thuma, M. Norton, *Microsc. Res. Tech.* **2000**, *48*, 367.
[48] P. Kayatz, G. Thumann, T. T. Luther, J. F. Jordan, K. U. Bartz-Schmidt, P. J. Esser, U. Schraermeyer, *Invest. Ophthalmol. Vis. Sci.* **2001**, *42*, 241.
[49] M. Elleder, J. Borovansky, *Histochem. J.* **2001**, *33*, 273.
[50] L. Mosca, C. De Marco, M. Fontana, M. A. Rosei, *Arch. Biochem. Biophys.* **1999**, *371*, 63.
[51] H. Nagaoka, S. Toyoshima, K. Takeda, *Anal. Sci.* **2002**, *18*, 951.
[52] L.-Q. Wu, H. Yi, S. Li, G. W. Rubloff, W. E. Bentley, R. Ghodssi, G. F. Payne, *Langmuir* **2003**, *19*, 519.

